Applied Physics Letters

A solution to the permalloy problem —A micromagnetic analysis with magnetostriction

Cite as: Appl. Phys. Lett. **118**, 212404 (2021); https://doi.org/10.1063/5.0051360
Submitted: 24 March 2021 • Accepted: 08 May 2021 • Published Online: 24 May 2021

Ananya Renuka Balakrishna and Richard D. James

Applied Physics Letters ARTICLE scitation.org/journal/apl

A solution to the permalloy problem—A micromagnetic analysis with magnetostriction

Cite as: Appl. Phys. Lett. **118**, 212404 (2021); doi: 10.1063/5.0051360
Submitted: 24 March 2021 · Accepted: 8 May 2021 ·
Published Online: 24 May 2021

Ananya Renuka Balakrishna[1,a] and Richard D. James[2]

AFFILIATIONS

[1]Aerospace and Mechanical Engineering, University of Southern California, Los Angeles California 90089, USA
[2]Aerospace Engineering and Mechanics, University of Minnesota, Minneapolis Minnesota 55455, USA

[a]Author to whom correspondence should be addressed: renukaba@usc.edu

ABSTRACT

A long-standing puzzle in the understanding of magnetic materials is the "Permalloy problem," i.e., why the particular composition of Permalloy, $Fe_{21.5}Ni_{78.5}$, achieves a dramatic drop in hysteresis and concomitant increase in initial permeability, while its material constants show no obvious signal of this behavior. In fact, the anisotropy constant κ_1 and the magnetostriction constants $\lambda_{100}, \lambda_{111}$ all vanish at various nearby, but distinctly different, compositions than $Fe_{21.5}Ni_{78.5}$. These compositions are in fact outside the compositional region where the main drop in hysteresis occurs. We use our newly developed coercivity tool [A. Renuka Balakrishna and R. D. James, Acta Mater. **208**, 116697 (2021)] to identify a delicate balance between local instabilities and magnetic material constants that lead to a dramatic decrease in coercivity at the Permalloy composition $Fe_{21.5}Ni_{78.5}$. Our results demonstrate that specific values of magnetostriction constants and anisotropy constants are necessary for the dramatic drop of hysteresis at 78.5% Ni. Our findings are in agreement with the Permalloy experiments and provide theoretical guidance for the development of other low hysteresis magnetic alloys.

In the early 20th century, an Fe–Ni alloy with unusually low coercivity was discovered at Bell Laboratories.[1] This magnetic alloy with precisely 78.5% Ni, now known as Permalloy, demonstrated a drastically lowered hysteresis, quantified by the value of coercivity, relative to nearby alloys (see Figs. 1(a)–1(d)). Several researchers attribute the dramatic decrease in hysteresis at 78.5% Ni to its small anisotropy constant κ_1—a material constant that quantifies the difficulty of rotating the magnetization away from certain preferred crystallographic axes.[2] However, a closer examination of the binary Fe–Ni alloys, containing 35% − 100% Ni, shows several peculiarities in behavior that contradict our current understanding of the origins of magnetic hysteresis (see Fig. 1(a)). For example, the anisotropy constant of the FeNi alloy is zero at 75% Ni; however, there is not even a local minimum of the coercivity vs composition at this Ni-content. However, at 78.5% Ni, where the anisotropy constant is clearly not zero, the coercivity is minimized.[3]

Besides the anisotropy constant, researchers have suspected that the magnetostriction constants, λ_{111} and λ_{100}, play some role in lowering magnetic hysteresis.[13,16,17] These magnetostriction constants relate the preferred strains corresponding to a given magnetization. The potential influence of λ_{100} is supported by the presence of the second Permalloy composition at 45% Ni, where the coercivity vs composition shows a diffuse local minimum, not nearly as sharp as in 78.5% Ni, but still clearly noticeable (see Figs. 1(b)–1(d)). The values of anisotropy constant κ_1 and magnetostriction constant λ_{111} are far from zero at 45% Ni, but the magnetostriction constant $\lambda_{100} = 0$ vanishes precisely at this composition. Following this line of argument, we would expect to see a lowering of hysteresis at 80% and 83% Ni, at which the magnetostriction constants λ_{111} and λ_{100} are zero, respectively. However, there is not even a discernible local minimum of coercivity vs composition at these compositions. By contrast, as mentioned above, the magnetic hysteresis is minimum at 78.5% Ni at which neither of the magnetostriction constants nor the anisotropy constant is zero. This collection of apparently contradictory facts is known as the "Permalloy problem."[3]

Processing also has an important influence on hysteresis. For example, slow cooling can raise the composition of the lowest hysteresis to higher Ni content.[2] Typically, the effect of a thermo-mechanical treatment in the Fe–Ni system is to induce the formation of precipitates. This, in turn, has two main effects: (a) it leads to the preferential deposition of one element into precipitates, which have a very different composition than the matrix. This precipitation causes a departure of the matrix composition from the nominal composition; and (b) it develops residual stress due to the geometric incompatibility of the

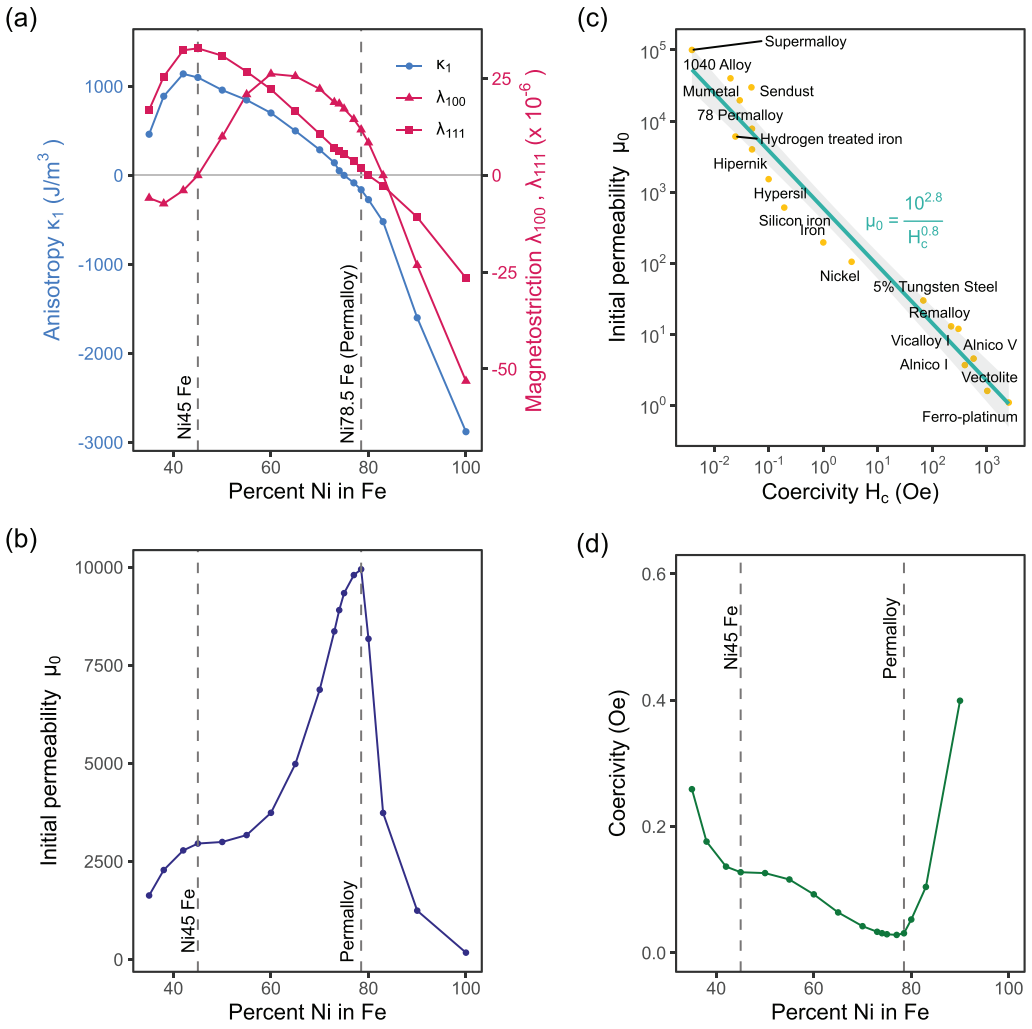

FIG. 1. (a) A plot of magnetic material constants, namely the anisotropy constant κ_1 and magnetostriction constants $\lambda_{100}, \lambda_{111}$, as a function of Ni content in Fe. (b) A permeability plot for Fe–Ni alloys as a function of Ni-content. The highest initial permeability is achieved at a 78.5% Ni-content, and a second peak is observed at a 45% Ni-content. (c) The initial permeability correlates inversely, $\mu_0 = 10^{2.8}/H_c^{0.8}$, with coercivity in magnetic alloys.[4] (d) Using subfigures (b) and (c), we estimate the relationship between Ni-content and coercivity in magnetic alloys. We note that the minimum coercivity is at a 78.5% Ni-content (Permalloy). Subfigure (a) is modified with permission from R. M. Bozorth, Rev. Mod. Phys. **25**(1), 42 (1953). Copyright 1953 American Physical Society. Subfigure (c) is modified with permission from C. Kittel, Rev. Mod. Phys. **21**(4), 541 (1949). Copyright 1949 American Physical Society.

precipitate and the matrix. This geometric incompatibility induces coherency stresses that affect magnetic properties via magnetostriction.[5,6] In certain systems, more disruptive processing treatments, such as rapid solidification leading to nanocrystalline materials,[7–9] engineering alloy compositions,[10] and designing magnetic nanoparticle geometries,[11,12] are also productive routes toward extremely low hysteresis materials.

Researchers have attempted to resolve the Permalloy problem for many years.[3,4,13,16] Domain theory has been used to explain the ease of domain rotation and domain wall movement at small values of anisotropy and magnetostriction constants.[16,17] These calculations make certain assumptions on magnetic microstructures and domain structures; however, these calculations do not predict low hysteresis at the Permalloy composition. In another study,[13] the criterion $|(\lambda_{100} - \lambda_{111})\sigma| = |\kappa_1|$ between magnetostriction and anisotropy constants (in the presence of residual stresses σ) is proposed as governing coercivity. While we agree with the importance of accounting for $\lambda_{100}, \lambda_{111}, \sigma$ and κ_1 in predicting coercivity, we do not see a fundamental theoretical or experimental basis for this criterion. In addition, since residual stress is a tensor varying with the position in a heterogeneous solid, it is not clear to us how to use this criterion. Several recent studies examine the effect of grain orientation and crystallographic texture on coercivity in soft magnetic alloys;[15,18,19] however, these studies do not address how fundamental material constants interact with defects and residual stress to lower hysteresis in this system.

In our paper, while recognizing that processing can be highly influential, we explore the hypothesis that there is a relation between hysteresis and fundamental material constants in the FeNi system. Doing so, we shed light on the Permalloy problem.

Recently, we developed a coercivity tool based on the micromagnetics theory.[28] Our tool differs from other theoretical methods that predict magnetic coercivity[22,24] in two ways: (a) first, we account for magnetoelastic interactions that have been neglected in most prior studies. (b) Second, we introduce an optimized localized disturbance in the form of a spike-domain microstructure that grows during magnetization reversal. By introducing the localized disturbance, we capture the delicate balance between magnetic material constants that govern hysteresis and predict coercivity with greater accuracy than other methods based on linear stability analysis. In this work, we apply this coercivity tool to provide insight into the Permalloy problem.

In this paper, we first provide an overview of the micromagnetics theory used in our coercivity tool. We then apply this tool in two studies on iron–nickel alloys: in study 1, we test the hypothesis that a specific combination of magnetoelastic constants (with residual stress) and anisotropy constants is necessary to lower the coercivity at the Permalloy composition. Here, we compute coercivity in iron–nickel alloys in two cases, (a) by accounting for magnetostrictive effects and (b) by ignoring all magnetoelastic energy contributions. In Study 2, we test the hypothesis that neither defect geometry nor defect orientation significantly affects the combination of material constants at which the lowest coercivity is achieved. Finally, we compare the magnetic coercivity predicted by the present study with previously proposed ideas.[16,17] Our simulations show that the lowest coercivity is attained at a 78.5% Ni-content when magnetoelastic energy is accounted for in the model and provides insight into minimum coercivity values of other Fe–Ni alloys.

Our coercivity tool is based on micromagnetics with magnetostriction.[20,21] The total free energy is a functional of magnetization $\mathbf{M}$, nondimensionalized as $\frac{\mathbf{M}}{m_s} = \mathbf{m} = m_1\mathbf{e}_1 + m_2\mathbf{e}_2 + m_3\mathbf{e}_3$, and strain $\mathbf{E} = \frac{1}{2}(\nabla\mathbf{u} + \nabla\mathbf{u}^T)$:

$$\Psi = \int_{\mathcal{E}} \Big\{ \nabla\mathbf{m}\cdot \mathrm{A}\nabla\mathbf{m} + \kappa_1(m_1^2m_2^2 + m_2^2m_3^2 + m_3^2m_1^2) + \frac{1}{2}[\mathbf{E} - \mathbf{E_0}(\mathbf{m})]\cdot\mathbb{C}[\mathbf{E} - \mathbf{E_0}(\mathbf{m})] - \boldsymbol{\sigma}_{\text{ext}}\cdot\mathbf{E} - \mu_0 m_s \mathbf{H}_{\text{ext}}\cdot\mathbf{m} \Big\} \mathrm{d}\mathbf{x} + \int_{\mathbb{R}^3} \frac{\mu_0}{2}|\mathbf{H}_{\mathrm{d}}|^2 \mathrm{d}\mathbf{x}, \tag{1}$$

and $\boldsymbol{\sigma}_{\text{ext}}, \mathbf{H}_{\text{ext}}$ are the (constant) applied stress and magnetic field, respectively. Here, the anisotropy energy $\kappa_1(m_1^2m_2^2 + m_2^2m_3^2 + m_3^2m_1^2)$ penalizes the rotation of the magnetization away from the easy axes, the elastic energy $\frac{1}{2}[\mathbf{E} - \mathbf{E_0}(\mathbf{m})]\cdot\mathbb{C}[\mathbf{E} - \mathbf{E_0}(\mathbf{m})]$ penalizes mechanical deformation away from the preferred strain, defined by

$$\mathbf{E_0}(\mathbf{m}) = \frac{3}{2}\begin{bmatrix} \lambda_{100}\left(m_1^2 - \frac{1}{3}\right) & \lambda_{111}m_1m_2 & \lambda_{111}m_1m_3 \\ & \lambda_{100}\left(m_2^2 - \frac{1}{3}\right) & \lambda_{111}m_2m_3 \\ symm. & & \lambda_{100}\left(m_3^2 - \frac{1}{3}\right) \end{bmatrix}. \tag{2}$$

Finally, the vector field $\mathbf{H}_{\mathrm{d}}$ is the stray field generated by the magnetization distribution, and the magnetostatic energy $\frac{\mu_0}{2}|\mathbf{H}_{\mathrm{d}}|^2$ is the energy required to assemble a collection of elementary magnetic dipoles into the given magnetization distribution.[23] The stray field $\mathbf{H}_{\mathrm{d}} = -\nabla\zeta_{\mathbf{m}}$ is obtained by solving the magnetostatic equation $\nabla\cdot(-\nabla\zeta_{\mathbf{m}} + \mathbf{M}) = 0$ on all of space. Here, we note that in this model, the five material constants $\mathrm{A}, \kappa_1, \lambda_{100}, \lambda_{111}, m_s$ together with the elastic modulus tensor $\mathbb{C}$ (depending on the three moduli c_{11}, c_{12}, c_{44}) and applied field and stress determine the form of the micromagnetic energy. See Ref. 28 for further explanation.

We compute the evolution of the magnetization using a local energy minimization technique, based on the generalized Landau–Lifshitz–Gilbert equation:[25]

$$\frac{\partial\mathbf{m}}{\partial\tau} = -\mathbf{m}\times\mathcal{H} - \alpha\mathbf{m}\times(\mathbf{m}\times\mathcal{H}). \tag{3}$$

Here, $\mathcal{H} = -\frac{1}{\mu_0 m_s^2}\frac{\delta\Psi}{\delta\mathbf{m}}$ is the effective field, $\tau = \gamma m_s t$ is the dimensionless time step, γ is the gyromagnetic ratio, and α is the damping constant. We numerically solve Eq. (3) using the Gauss Siedel projection method[26] and identify equilibrium states when the magnetization evolution converges, $|\mathbf{m}^{n+1} - \mathbf{m}^n| < 10^{-9}$. At each iteration, we compute the magnetostatic field $\mathbf{H_d} = -\nabla\zeta_{\mathbf{m}}$ and the strain $\mathbf{E}$ by solving their respective equilibrium equations:

$$\nabla\cdot(-\nabla\zeta_{\mathbf{m}} + \mathbf{M}) = 0 \quad \text{on } \mathbb{R}^3, \tag{4}$$

$$\nabla\cdot\mathbb{C}(\mathbf{E} - \mathbf{E}_0) = 0. \tag{5}$$

The magnetostatic equilibrium condition arises from the Maxwell equations, namely $\nabla\times\mathbf{H_d} = 0 \rightarrow \mathbf{H_d} = -\nabla\zeta_{\mathbf{m}}$ and $\nabla\cdot\mathbf{B} = \nabla\cdot(\mathbf{H_d} + \mathbf{M}) = 0$. We compute the magnetostatic and mechanical equilibrium conditions in Eqs. (4) and (5) in Fourier space.[27] Further details on the numerical method can be found in Refs. 26–28.

In the present work, we calibrate our micromagnetics model for the FeNi alloy as a function of the Ni-content. The material constants used in our calculations are listed in the supplementary material. We assume an ellipsoid under a suitably oriented applied field (see Fig. 2(a)). Note that the applied field is directed along the major axis of the magnetic ellipsoid. The easy axes for Fe–Ni alloys with anisotropy constants $\kappa_1 > 0$ and $\kappa_1 < 0$ are along $\langle 100\rangle$ and $\langle 111\rangle$ crystallographic directions, respectively. This ellipsoid is uniformly magnetized except at the proximity of defects. Using a computational scheme based on the ellipsoid and reciprocal theorems, we model a 3D computational domain Ω with a nonmagnetic inclusion at its geometric center. That is, in our method, the presence of the large ellipsoidal body $\mathcal{E}$ is essential as a way of describing the poles on the boundary of the macroscale body without having to simulate the external fields due to these poles.[28] The domain and the inclusion are of sizes $64\times64\times24$ and $12\times12\times6$ grid points. The cell size is chosen such that the domain walls span across 3–4 elements. The magnetization inside the inclusion is held at zero throughout the computation, $|\mathbf{m}| = 0$. Outside the defect, we initialize the computation domain with a uniform magnetization $\mathbf{m} = \mathrm{m}_1\mathbf{e}_1$, and apply a large external field along the easy axes, $\mathbf{H}_{\text{ext}} \gg 0$ (see Fig. 2(b)). As we decrease the applied field, the spike domain at first grows slowly until a critical field is reached at which the magnetization vector reverses abruptly. We identify this value of the applied field with coercivity. We use this approach to predict the coercivity of the iron–nickel alloys as a function of the Ni-content.

In Study 1, we test our hypothesis that the magnetoelastic energy contributions (e.g., magnetostrictive and residual stress), in addition to

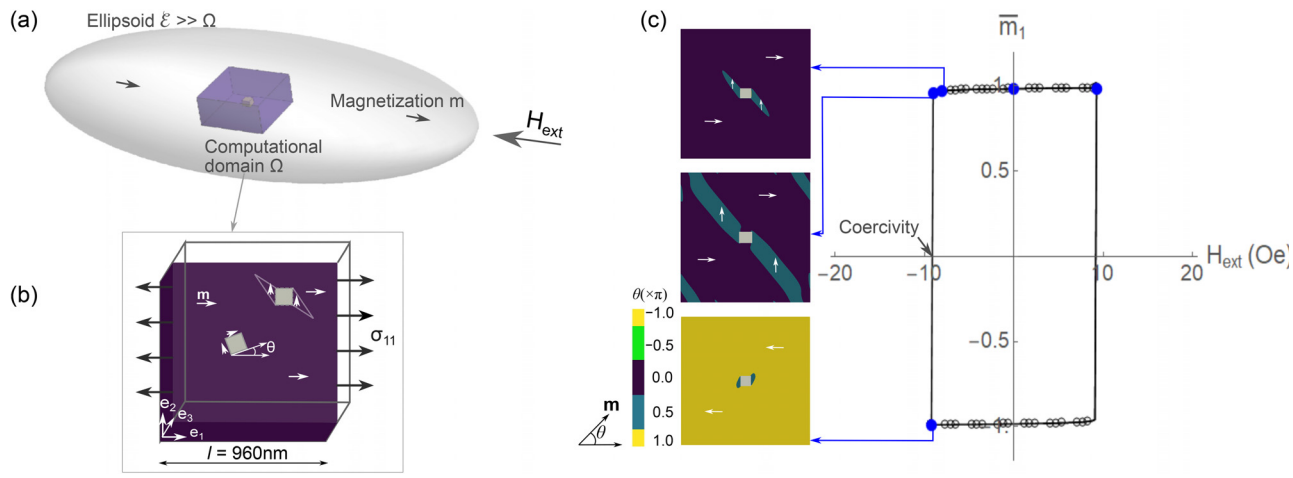

FIG. 2. (a) A schematic illustration of an ellipsoid $\mathcal{E}$ with uniform magnetization **m**. We apply an external field H_{ext} to reverse the magnetization in the ellipsoid and compute its coercivity. (b) In our computations, we mode a 3D computational domain Ω with nonmagnetic inclusions. This computational domain of size $l = 960$nm is much smaller than the size of the ellipsoid $\mathcal{E} \gg \Omega$. Other parameters modeled in the present study, such as defect orientation θ and applied stresses σ_{11} and external field $\mathbf{H}_{ext}$, are schematically illustrated. (c) A representative calculation of magnetic coercivity. We apply a large external field H_{ext} in the direction of magnetization and decrease its value incrementally. At a critical field strength, known as coercivity, the magnetization reverses. The inset figures show microstructures during magnetization reversal, and the color bar represents the orientation of magnetization.

the anisotropy energy, are necessary to reproduce the characteristic features of coercivity vs composition in iron–nickel alloys. To test this hypothesis, we compute the coercivity for iron–nickel alloys in two cases: (a) by accounting for the magnetoelastic energy with small residual stress $\sigma_{11} = 5$ MPa and (b) by ignoring all magnetoelastic energy in Eq. 1. Note that a residual stress of $\sigma_{11} = 5$ MPa corresponds to a uniaxial strain of about 25 $\mu\epsilon$ (with typical Young's modulus of about 200 GPa) for Fe–Ni alloys. As noted above, these residual stresses naturally arise from precipitation during heat treatment and from other defects such as the presence of grain boundaries and, in particular, triple junctions. For example, a temperature change of 1 K causes about $10\mu\epsilon$ strain in iron. Our assumption of $25\mu\epsilon$ residual strains is well within the thermal strain for moderate temperature changes.

Figure 3(a) shows the coercivity of iron–nickel alloys for the two cases. In line with the experimental evidence, the coercivity is the lowest at a 78.5% Ni-content when both magnetoelastic and anisotropy energy contributions are accounted in the free energy function. When magnetoelastic energy is neglected (or small), the coercivity is minimum at a 75% Ni-content at which $\kappa_1 = 0$. Similarly, our calculations show that the coercive field has a local minimum at 45% − 50% Ni-content, when both magnetoelastic and anisotropy energy contributions are included in the model. Furthermore, this minimum is more pronounced with increased stresses in the material (see Fig. 3(b)). Although the anisotropy constant is large in this composition range $\kappa_1 \approx 10^3 \mathrm{J/m}^3$, we find that its coercivity is relatively small in this neighborhood. This is consistent with experiments, in which the permeability peaks are observed at the 45% and 78.5% Ni-contents, respectively, and with previous hypotheses by researchers,[3,14] who speculated that the low magnetostriction constant $\lambda_{100} \to 0$ in the $45\% \leq \mathrm{Ni} \leq 50\%$ neighborhood causes a local minimum (or maximum) in the Fe–Ni coercivity (or permeability) plot. When $\lambda_{100} = 0$, the strain values are decoupled from the magnetization vector, and consequently, the residual stresses do not affect the coercivity values.

In Study 2, we test our hypothesis that neither defect geometries nor defect densities affect the balance between material constants at which minimum coercivity is achieved. Figures 3(c) and 3(d) show the effect of defect geometry (such as orientation and shape) and density on the coercivity of the Fe–Ni alloy. Note that these computations were modeled with a residual stress of $\sigma_{11} = 5$ MPa. The magnitude of the coercivity is sensitive to defect geometries and tensile stresses; however, as hypothesized, for a given defect configuration, the minimum coercivity remains at a 78.5% Ni-content. The balance between anisotropy and magnetostriction constants that minimizes the coercivity at a 78.5% Ni-content is not significantly affected by the changes in defect geometry and/or orientation. These results are consistent with a wider set of variations of defect size and placement presented in Ref. 28 (but not for material constants of Permalloy). Furthermore, our results are consistent with independent experiments that report the lowest coercivity at the Permalloy composition (despite differences in manufacturing techniques, defect geometries, and/or polycrystalline microstructures).[2,3,30,31]

We next compare our findings with predictions from domain theory and Lewis criterion.[13,16,17] We do not include results from the linear stability analysis of the single domain state based on micromagnetics because these vastly over-predict the coercivity. (This overprediction is known as the "coercivity paradox." Our simulations are outside the regime of linear stability analysis.) We compare our results with prior predictions by choosing specific compositions of the iron–nickel alloys (e.g., alloys with 45, 75, 78.5, 80, and 83% Ni-contents) to highlight the zeros of the material constants (see the supplementary material): we note that the formulas from domain theory $\mu_0|_{\kappa_1} \approx \frac{2m_s^2}{\kappa_1}$ or $\mu_0|_{\lambda} \approx \frac{5m_s^2}{\lambda^2 E}$ predict large permeabilities $(\to \infty)$ at multiple singularities; however, they fail to identify the highest permeability (lowest coercivity) at the 78.5% Ni-content alloy. For example, domain theory predicts the highest permeability at a 75% Ni-content with $\kappa_1 = 0$ and at a 45% Ni-content with $\lambda_{100} = 0$; however, experiments indicate that

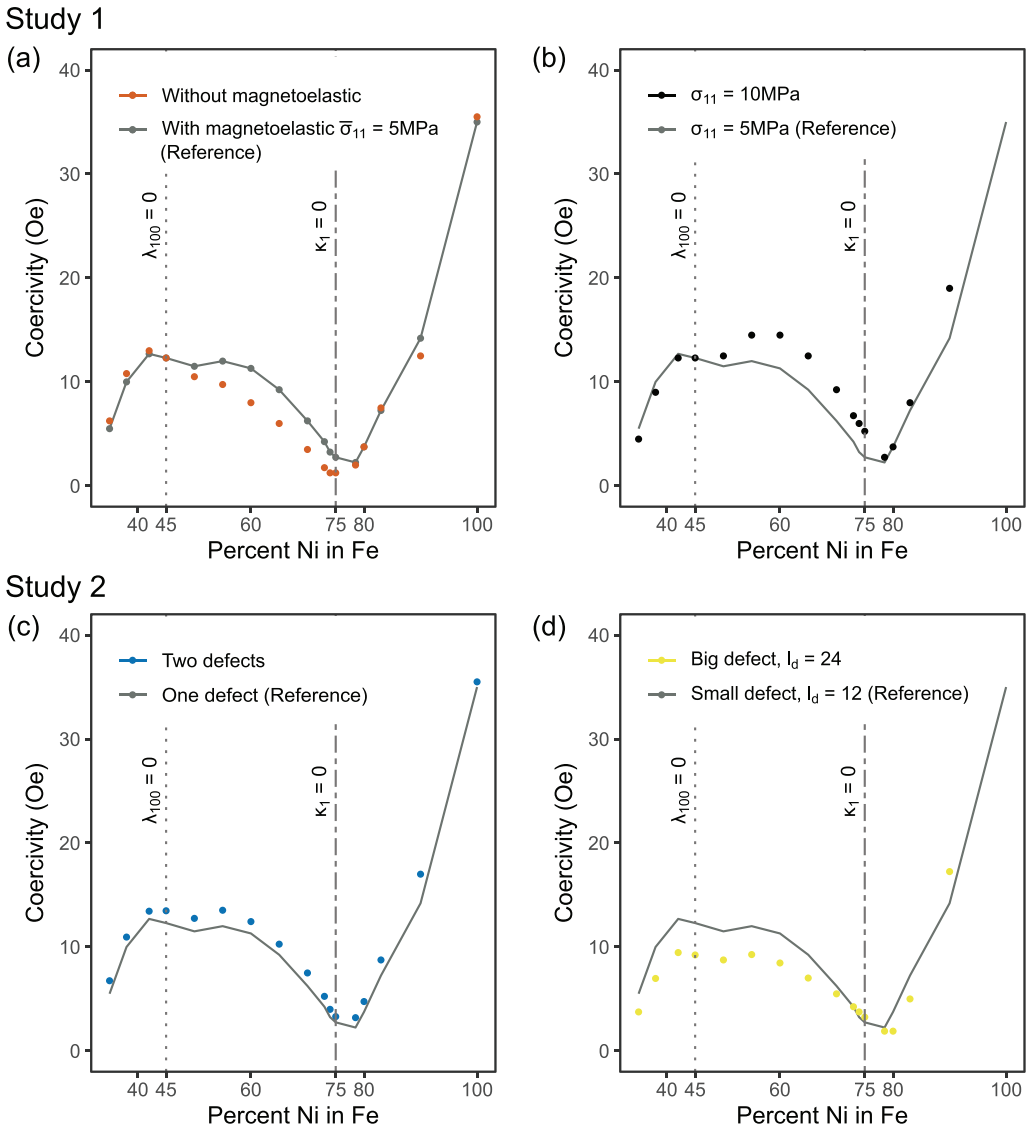

FIG. 3. Computed coercivity values in iron–nickel alloys as a function of Ni-content in (a) and (b) Study 1 and (c) and (d) Study 2. (a) When both the anisotropy and magnetoelastic energies (including residual stresses σ_{11}) are accounted for in the free energy function, the lowest coercivity is predicted at a 78.5% Ni-content. When magnetoelastic energy is neglected and only anisotropy energy is accounted in the free energy function, the lowest coercivity is predicted at a 75% Ni-content. (b) The minima at 78.5% and 45% Ni-content alloys are more pronounced in iron–nickel alloys under tensile stresses, for example, $\sigma_{11} = 10$ MPa. The reference plot corresponds to the coercivity values of Fe–Ni alloys with magnetoelastic interactions and residual stresses $(\lambda_{100}, \lambda_{111}, \sigma_{11})$ in subfigure 2(a) and (c) defect orientation and density affect the coercivity values; however, their effect is small. (d) The size of the defect modeled on the computational domain also affects coercivity values in Fe–Ni alloys.

the highest permeability occurs at a 78.5% Ni-content at which neither κ_1 nor λ_{100} is zero. Similarly, the Lewis criterion $|(\lambda_{100} - \lambda_{111})\sigma| = |\kappa_1|$ is closely satisfied at a 75% Ni-content with a value $\sigma = 5$ MPa; however, it misses the dramatic drop in coercivity at the 78.5% alloy composition. Furthermore, it is unclear on how to choose the residual stress σ in the criterion; we keep it at $\sigma = 5$ MPa to reflect the fact that the measured values were obtained from alloys with nominally the same heat treatment. By contrast, our coercivity tool predicts the highest permeability (or lowest coercivity) at a 78.5% Ni-content (see Figs. 3(a) and 3(b)). Furthermore, it shows a local minimum in coercivity at 45% Ni and provides insight into coercivities at other alloy compositions with zero material constants. Our predictions are consistent with the experimentally measured permeability values for Fe–Ni alloys (see Fig. 1).[3] Overall, the prior criteria or formulas that explain the low coercivity at the Permalloy composition are not general and do not fully explain the singularities at other material compositions. These results suggest that our approach based on non-linear stability analysis at the shoulder of the hysteresis loop together with a delicate balance of magnetic material constants is a potential way forward to reliably predict coercivities.

In summary, our findings on coercivity as a function of the Ni-content in the binary Fe–Ni alloys show that the lowest coercivity is attained at a 78.5% Ni-content. This was the case in Study 1 when both anisotropy and magnetoelastic energy contributions were included in the calculations. In Study 2, although tensile stresses and defect geometries affected the coercivity values, the minimum coercivity was still observed at a 78.5% Ni-content. Furthermore, our predictions on coercivity as a function of the Ni-content are more accurate than prior criteria based on domain theory and provide insight into the Permalloy problem. Below, we discuss some limiting conditions on our results and then highlight the key features of our work.

Two features of this work limit the conclusions we can draw regarding the Permalloy problem. First, we assume a single crystalline ellipsoid body, which does not contain grain boundaries, sharp edges, and other imperfections, which are commonly found in bulk magnetic materials. This assumption possibly contributes to about an order of magnitude difference between our predicted coercivity values and those reported from experiments. Second, we model the local disturbance (spike domain) explicitly by defining a potent defect on the computational domain. Whether developing a more fundamental theory of nucleation in the Calculus of Variations without explicitly defining the nucleus would provide further insights into magnetic coercivity is an open question. With these reservations in mind, we next discuss our findings on the Permalloy problem.

The key feature of our work is that we show a delicate balance between material constants, $\kappa_1, \lambda_{100}, \lambda_{111}$, and is necessary for the low coercivity at a 78.5% Ni-content. This finding contrasts with some reports in the literature in which the small anisotropy constant $\kappa_1 \to 0$ is considered to be the *only* factor responsible for lowering hysteresis. Although $\kappa_1 = 0$ lowers the coercivity (e.g., at a 75% Ni-content), we find that magnetostriction plays an important role in governing magnetic hysteresis. Furthermore, our findings are consistent with previous hypotheses that the zero magnetostriction constants—along the easy axes—at 45% and 80% Ni-contents help lower the coercivity values. Despite the large anisotropy constants at these compositions, we find that their coercivities are relatively small in their local Ni-content neighborhoods.

Another feature of our work is that we propose a theoretical method to compute coercivity, on the shoulder of the hysteresis loop, by accounting for localized instabilities (spike domain). This approach of computing non-linear stability analysis helped us to elucidate the role of magnetic material constants on coercivity. We believe that this method helped us to predict coercivities more accurately when compared to other methods that are based on linearization. In our future work, we use our tool to compute coercivity in a broader material parameter space[29] and seek to identify the fundamental relation between the material constants that govern hysteresis.

To conclude, the present findings contribute to a more nuanced understanding of how material constants, such as anisotropy and magnetostriction constants, affect magnetic hysteresis. Specifically, magnetoelastic interactions have been regarded to play a negligible role in lowering the coercivity. Given the current findings, we quantitatively demonstrate that the interplay between anisotropy energy, magnetoelastic energy, and localized disturbance (spike domain) is necessary to lower magnetic hysteresis. Our theoretical model serves as a design tool to discover novel combinations of material constants, which lower the coercivity in magnetic alloys.

See the supplementary material for a complete list of Fe–Ni alloy's material constants.

The authors acknowledge the Center for Advanced Research Computing at the University of Southern California and the Minnesota Supercomputing Institute at the University of Minnesota for providing resources that contributed to the research results reported within this paper. A.R.B acknowledges the support of a Provost Assistant Professor Fellowship, Gabilan WiSE fellowship, and USC's start-up funds. R.D.J acknowledges the support of a Vannevar Bush Faculty Fellowship. The authors thank NSF (No. DMREF-1629026) and ONR (No. N00014-18-1-2766) for partial support of this work.

DATA AVAILABILITY

The data that support the findings of this study are available within the article and its supplementary material.

REFERENCES

[1]H. D. Arnold and G. W. Elmen, "Permalloy, an alloy of remarkable magnetic properties," J. Franklin Inst. **195**(5), 621–632 (1923).
[2]R. M. Bozorth, *Ferromagnetism* (Piscataway, NJ, 1978).
[3]R. M. Bozorth, "The permalloy problem," Rev. Mod. Phys. **25**(1), 42 (1953).
[4]C. Kittel, "Physical theory of ferromagnetic domains," Rev. Mod. Phys. **21**(4), 541 (1949).
[5]J. Fidler, "Coercivity of precipitation hardened cobalt rare earth 17: 2 permanent magnets," J. Magn. Magn. Mater. **30**(1), 58–70 (1982).
[6]M. Sagawa, M. Okada, and Z. Henmi, "The relation between precipitation and coercivity in Co-Fe-Nb semihard magnetic alloy," Trans. Jpn. Inst. Met. **17**(10), 615–619 (1976).
[7]F. Jiménez-Villacorta, J. L. Marion, J. T. Oldham, M. Daniil, M. A. Willard, and L. H. Lewis, "Magnetism-structure correlations during the $\epsilon \to \tau$ transformation in rapidly-solidified MnAl nanostructured alloys," Metals **4**(1), 8–19 (2014).
[8]M. E. McHenry, M. A. Willard, and D. E. Laughlin, "Amorphous and nanocrystalline materials for applications as soft magnets," Prog. Mater. Sci. **44**(4), 291–433 (1999).
[9]J. Rial, M. Villanueva, E. Céspedes, N. López, J. Camarero, L. G. Marshall, L. H. Lewis, and A. Bollero, "Application of a novel flash-milling procedure for coercivity development in nanocrystalline MnAl permanent magnet powders," J. Phys. D: Appl. Phys. **50**(10), 105004 (2017).
[10]L. Jiang, J. Yang, H. Hao, G. Zhang, S. Wu, Y. Chen, O. Obi, T. Fitchorov, and V. G. Harris, "Giant enhancement in the magnetostrictive effect of FeGa alloys doped with low levels of terbium," Appl. Phys. Lett. **102**(22), 222409 (2013).
[11]D. X. Niu, X. Zou, J. Wu, and Y. B. Xu, "Anisotropic magnetization reversal in 30 nm triangular FeNi dots," Appl. Phys. Lett. **94**(7), 072501 (2009).
[12]Y. Liu, S. Gliga, R. Hertel, and C. M. Schneider, "Current-induced magnetic vortex core switching in a Permalloy nanodisk," Appl. Phys. Lett. **91**(11), 112501 (2007).
[13]B. Lewis, "The permalloy problem and anisotropy in nickel iron magnetic films," Br. J. Appl. Phys. **15**(5), 531 (1964).
[14]R. D. James, "Magnetic alloys break the rules," Nature **521**(7552), 298–299 (2015).
[15]K. Suzuki, G. Herzer, and J. M. Cadogan, "The effect of coherent uniaxial anisotropies on the grain-size dependence of coercivity in nanocrystalline soft magnetic alloys," J. Magn. Magn. Mater. **177–181**, 949–950 (1998).
[16]R. Becker and W. Doring, *Ferromagnetismus*, edited by J. W. Edwards (Julius Springer, Berlin, 1939).
[17]C. Kittel and J. K. Galt, "Ferromagnetic domain theory," in *Solid State Physics* (Academic Press, 1956), Vol. 3, pp. 437–564.
[18]A. E. M. A. Mohamed, J. Zou, R. S. Sheridan, K. Bongs, and M. M. Attallah, "Magnetic shielding promotion via the control of magnetic anisotropy and

thermal Post processing in laser powder bed fusion processed NiFeMo-based soft magnet," Addit. Manuf. **32**, 101079 (2020).
[19]J. Zou, Y. Gaber, G. Voulazeris, S. Li, L. Vazquez, L. F. Liu, M. Y. Yao, Y. J. Wang, M. Holynski, K. Bongs, and M. M. Attallah, "Controlling the grain orientation during laser powder bed fusion to tailor the magnetic characteristics in a Ni-Fe based soft magnet," Acta Mater. **158**, 230–238 (2018).
[20]W. F. Brown, *Micromagnetics (No. 18)* (Interscience Publishers, 1963).
[21]W. F. Brown, *Magnetoelastic Interactions* (Springer, Berlin, 1966), Vol. 9.
[22]M. Kruzík and A. Prohl, "Recent developments in the modeling, analysis, and numerics of ferromagnetism," SIAM Rev. **48**(3), 439–483 (2006).
[23]R. D. James and S. Müller, "Internal variables and fine-scale oscillations in micromagnetics," Continuum Mech. Thermodyn. **6**(4), 291–336 (1994).
[24]L. Lopez-Diaz, D. Aurelio, L. Torres, E. Martinez, M. A. Hernandez-Lopez, J. Gomez, O. Alejos, M. Carpentieri, G. Finocchio, and G. Consolo, "Micromagnetic simulations using graphics processing units," J. Phys. D: Appl. Phys. **45**(32), 323001 (2012).
[25]T. L. Gilbert, "A phenomenological theory of damping in ferromagnetic materials," IEEE Trans. Magn. **40**(6), 3443–3449 (2004).
[26]X. P. Wang, C. J. Garcia-Cervera, and E. Weinan, "A Gauss-Siedel projection method for micromagnetics simulations," J. Comput. Phys. **171**(1), 357–372 (2001).
[27]J. X. Zhang and L. Q. Chen, "Phase-field microelasticity theory and micromagnetic simulations of domain structures in giant magnetostrictive materials," Acta Mater. **53**(9), 2845–2855 (2005).
[28]A. R. Balakrishna and R. D. James, "A tool to predict coercivity in magnetic materials," Acta Mater. **208**, 116697 (2021).
[29]A. R. Balakrishna and R. D. James, "Design of soft magnetic materials," Preprint (2021).
[30]X. Su, H. Zheng, Z. Yang, Y. Zhu, and A. Pan, "Preparation of nanosized particles of FeNi and FeCo alloy in solution," J. Mater. Sci. **38**(22), 4581–4585 (2003).
[31]S. J. Rosenberg, *Nickel Its Alloys* (US Department of Commerce, National Bureau of Standards, 1968), Vol. 106.